Physical Properties of the Weak-Ferromagnetic Superconductor $RuSr_2EuCu_2O_8$

B. C. Chang,[1] C. Y. Yang,[1] H. C. Ku,[1,*] J. C. Ho,[2]
C. B. Tsai,[3] Y. Y. Chen,[3] and D. C. Ling[4]

[1]*Department of Physics, National Tsing Hua University, Hsinchu 30013, Taiwan, Republic of China*
[2]*Department of Physics, Wichita State University, Wichita, Kansas 67260-0032, U.S.A.*
[3]*Institute of Physics, Academia Sinica, Taipei 11529, Taiwan, Republic of China*
[4]*Department of Physics, Tamkang University, Tamsui 25137, Taiwan, Republic of China*

(Received August 26, 2008)

Similar to the optimal-doped, weak-ferromagnetic (WFM induced by canted antiferromagnetism, $T_{\rm Curie}$ = 131 K) and superconducting ($T_{\rm c}$ = 56 K) $RuSr_2GdCu_2O_8$, underdoped $RuSr_2EuCu_2O_8$ ($T_{\rm Curie}$ = 133 K, $T_{\rm c}$ = 36 K) also exhibited a spontaneous vortex state (SVS) between 16 K and 36 K. The low field (±20 G) superconducting hysteresis loop indicates a weak and narrow Meissner state region of average lower critical field $B_{c1}^{\rm ave}(T) = B_{c1}^{\rm ave}(0)[1 - (T/T_{\rm SVS})^2]$, with $B_{c1}^{\rm ave}(0)$ = 7 G and $T_{\rm SVS}$ = 16 K. The vortex melting transition ($T_{\rm melting}$ = 21 K) below $T_{\rm c}$, obtained from the broad resistivity drop and the onset of the diamagnetic signal, indicates a vortex liquid region due to the coexistence and interplay between superconductivity and the WFM order. No visible jump in specific heat was observed near $T_{\rm c}$ for Eu- and Gd-compounds. Finally, with the baseline from the nonmagnetic Eu-compound, the specific heat data analysis confirms the magnetic entropy associated with antiferromagnetic ordering of Gd^{3+} ($J = S = 7/2$) at 2.5 K to be close to $N_{\rm A}k \ln 8$, as expected.

PACS numbers: 74.72.-h, 74.70.Pq, 74.25.Bt

I. INTRODUCTION

Anomalous physical properties have been observed recently in the weak-ferromagnetic (WFM induced by canted antiferromagnetism) and high-$T_{\rm c}$ superconducting $RuSr_2RCu_2O_8$ system (Ru-1212 with R = Sm, Eu, Gd, and Y) having a tetragonal $TlBa_2CaCu_2O_7$-type structure [1–48]. Possible superconductivity was also reported in Ca-substituted WFM compounds $RuCa_2RCu_2O_8$ (R = Pr-Gd) [49–51]. The weak-ferromagnetism in these strongly-correlated electron systems originates from the long range order of Ru moments in the RuO_6 octahedra due to a strong Ru-4$d_{xy,yz,zx}$-O-2$p_{x,y,z}$ hybridization with a Curie temperature $T_{\rm Curie} \sim$ 131 K. A G-type antiferromagnetic order probably occurs with the Ru^{5+} moment μ canted along the tetragonal basal plane, even through the small net spontaneous magnetic moment $\mu_s \ll \mu(Ru^{5+})$ is too small to be detected in neutron diffraction [4, 5, 9, 10, 22]. The Ru valence of 4+ and 5+ was determined from X-ray absorption near the edge measurements [23, 52].

With its quasi-two-dimensional CuO_2 bi-layers separated by a rare earth layer in the Ru-1212 structure, $RuSr_2GdCu_2O_8$ has the highest resistivity-onset temperature $T_c \sim 60$ K among the different Ru-1212 compounds [1, 2, 4, 5, 31]. A broad resistivity transition width, $\Delta T_c = T_c(\text{onset}) - T_c(\text{zero}) = T_c - T_{\text{melting}} \sim$ 15–20 K, is most likely a consequence of the coexistence and interplay between the superconductivity and WFM order. The diamagnetic signal is observed only near T_{melting} instead of T_c, and a reasonable large Meissner signal can be detected only in the zero-field-cooled (ZFC) mode [47]. Lower $T_c \sim 40$ K and 12 K were observed for the Eu-compound and Sm-compound, respectively [12, 18]. No superconductivity can be detected in $RuSr_2RCu_2O_8$ (R = Pr, Nd) [3, 16], while a superconducting $RuSr_2YCu_2O_8$ phase is stable only under high pressure [21, 26].

Interest in the current work was stimulated from a recent report of a spontaneous vortex state (SVS) between 30 K and 56 K in $RuSr_2GdCu_2O_8$ [47]. However, the compound undergoes a low temperature antiferromagnetic ordering arising from Gd^{3+} at 2.5 K. To avoid this complication, isostructural $RuSr_2EuCu_2O_8$ with nonmagnetic-Eu^{3+} ions was chosen as a prototype material in this study to evaluate the anomalous magnetic, transport, and calorimetric properties and the *d*-wave nature near and below $T_c = 36$ K. The calorimetric data were further used as a basis in elucidating the magnetic entropy associated with the Gd^{3+} ordering.

II. EXPERIMENT

Stoichiometric $RuSr_2RCu_2O_8$ samples were synthesized by solid-state reactions. High-purity RuO_2 (99.99%), $SrCO_3$ (99.9%), R_2O_3 (99.99%) (R = Pr, Nd, Sm, Eu, and Gd), and CuO (99.9%), in the nominal composition ratios of Ru:Sr:R:Cu = 1: 2: 1: 2, were well mixed and calcined at 960° C in air for 16 hours. The calcined powders were then pressed into pellets and sintered in flowing N_2 gas at 1015° C for 10 hours to form $RuSr_2RO_6$ and Cu_2O precursors. This step is crucial in order to avoid the formation of impurity phases. The N_2-sintered pellets were heated at 1060° C in flowing O_2 gas for 10 hours to form the Ru-1212 phase, then oxygen-annealed at a slightly higher temperature, 1065° C, for 7 days and slowly furnace-cooled to room temperature at a rate of 15° C per hour [47].

Powder X-ray diffraction data were collected with a Rigaku Rotaflex 18-kW rotating-anode diffractometer using Cu-K_α radiation. Four-probe electrical resistivity measurements were performed with a Linear Research LR-700 ac (16Hz) resistance bridge from 2 K to 300 K. Magnetic susceptibility and magnetic hysteresis measurements from 2 K to 300 K in low applied magnetic fields were carried out with a Quantum Design μ-metal shielded MPMS2 superconducting quantum interference device (SQUID) magnetometer. Calorimetric measurements were made from 1 K to 70 K by using a thermal-relaxation microcalorimeter. A mg-size sample was attached with a minute amount of grease to a sapphire holder to ensure good thermal coupling. The sample holder had a Cernox temperature sensor and a Ni-Cr alloy film heater. The holder was linked thermally to a copper block by four Au-Cu alloy

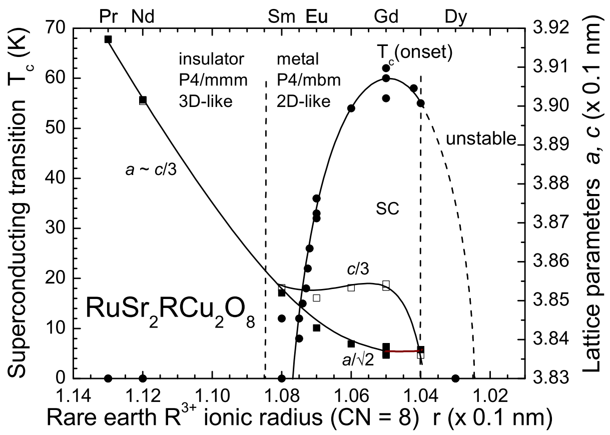

FIG. 1: The variation of the superconducting transition T_c and tetragonal lattice parameters a, c with the rare earth ionic radius R^{3+} (coordination number CN = 8) for the $RuSr_2RCu_2O_{8-\delta}$ system (R = Pr-Y).

wires. The temperature of the block could be raised in steps, but was held constant when a heat pulse was applied. Following each heat pulse, the sample temperature relaxation rate was monitored to yield a time constant τ. The total heat capacity was calculated from the expression $c = \kappa\tau$, where κ is the thermal conductance of Au-Cu wires. The heat capacity of the holder was measured separately for addenda correction. The molar specific heat of the sample was then obtained from $C = (c - c_{\text{addenda}})/(m/M)$ with m and M being the sample's mass and molar mass, respectively.

III. RESULTS AND DISCUSSION

Figure 1 summarizes the structural and superconducting properties as a function of R^{3+} the ionic radius r (coordination number CN = 8) of various $RuSr_2RCu_2O_{8-\delta}$ systems (R = Pr-Y). T_c decreases from a maximum value of 60 K for optimal-doped Gd ($r = 0.105$ nm) to 36 K for underdoped Eu ($r = 0.107$ nm), and is < 10 K for Sm ($r = 0.108$ nm). The larger rare earth ions of Nd (0.112 nm) and Pr (0.113 nm) lead to a metal-insulator transition. A powder X-ray Rietveld refinement study indicates that the insulating phase is stabilized in the undistorted tetragonal phase (space group P4/mmm) with a larger lattice parameter $a \sim 0.390$–392 nm, which gives a reasonable Ru^{5+}-O bond length of $d \sim 0.197$ nm if the oxygen content is slightly deficient ($\delta > 0$). On the other hand, the metallic phase with smaller rare earth ions can be stabilized in the full-oxygenated ($\delta \sim 0$), distorted tetragonal phase (space group P4/mbm) with smaller $a/\sqrt{2} \sim 0.383$–0.385 nm but still a reasonable Ru-O bond length through RuO_6 octahedron rotation.

Indeed, the powder X-ray diffraction pattern for the oxygen-annealed

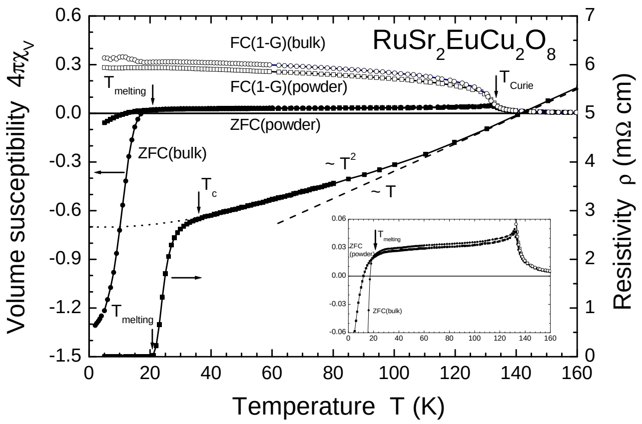

FIG. 2: The electrical resistivity $\rho(T)$ and volume magnetic susceptibility $4\pi\chi_V(T)$ in 1-G field-cooled (FC) and zero-field-cooled (ZFC) modes for oxygen-annealed bulk and powder $RuSr_2EuCu_2O_8$ samples.

$RuSr_2EuCu_2O_{8-\delta}$ sample indicates a single phase with tetragonal lattice parameters of $a = 0.5435(5)$ nm and $c = 1.1552(9)$ nm. A Raman scattering peak of 265 cm^{-1} indicates that the A_{1g} mode symmetry belongs to the P4/mbm instead of the P4/mmm group. Accordingly, with a RuO_6 octahedra rotation angle $\theta \sim 14^\circ$ around the c-axis and oxygen parameter $\delta \sim 0$ [10], the Rietveld refinement analysis with a small residual error factor $R = 5.31\%$ yields reasonable Ru-O bond lengths $d = (a/2\sqrt{2})(1-\sin^2\theta)^{-1/2} = 0.198$ nm. This is close to the minimum calculated bond length $d(Ru^{5+}\text{-}O)$ of 0.197 nm [10].

Figure 2 shows the temperature dependence of the field-cooled (FC) and zero-field-cooled (ZFC) volume magnetic susceptibility $4\pi\chi_V$ at 1-G for bulk and powder $RuSr_2EuCu_2O_8$ samples. Weak-ferromagmagnetic ordering occurs at $T_{\rm Curie} = 133$ K. Similar to $RuSr_2GdCu_2O_8$ [47]. This Eu-compound has its electrical resistivity data, which are also included in Fig. 2, exhibiting a non-Fermi-liquid-like behavior above $T_{\rm Curie}$. The linearly temperature-dependant values of 10.0 mΩ cm at 300 K and 5.5 mΩ cm at 160 K give an extrapolated value of 2.6 mΩ cm at 0 K, yielding a ratio $\rho(300\text{ K})/\rho(0\text{ K})$ of 3.9. Below $T_{\rm Curie}$, a T^2 behavior prevails. The onset of deviation at 36 K from such a temperature dependence is taken as the superconducting transition temperature $T_{\rm c}$. The melting temperature of the superconducting vortex liquid is assigned to be $T_{\rm melting} = 21$ K, where the resistivity reaches zero [47]. The broad transition width of 15 K is the common feature for all reported Ru-1212 compounds. The resistivity is sensitive to the granularity of polycrystalline samples, and the value of $T_{\rm c}$ is highly dependent on the details of synthesis and annealing. Thus the broad transition in the Ru-1212 compound may indicate a large inhomogeneity in the sample.

The Meissner shielding at 2 K is complete ($4\pi\chi_V = 4\pi M/B_a \sim 1.3$) for the ZFC bulk sample, but much reduced (-0.1) in the powder sample. The ZFC data curve looks like that of a mixed state, and the locally internal magnetic field is not completely expelled. However, in the 1-G FC mode, no diamagnetic signal can be detected below $T_{\rm melting}$. The

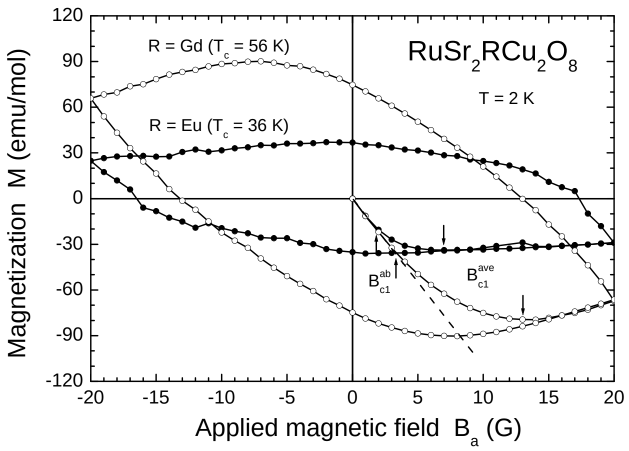

FIG. 3: The low-field superconducting hysteresis loops $M - B_a$ at 2 K for $RuSr_2GdCu_2O_8$ and $RuSr_2EuCu_2O_8$. The average lower critical field B_{c1}(ave) at the peak values and *ab*-plane B_{c1}^{ab} for deviation from initial linear lines are indicated by arrows.

lack of diamagnetism in the 1-G FC data below T_c is a common characteristic of a magnetic superconductor with a low critical current density J_c.

Low-field (±20 G) superconducting hysteresis loops at 2 K for a bulk sample $RuSr_2EuCu_2O_8$ and $RuSr_2GdCu_2O_8$ as reference are shown in Fig. 3. The initial magnetization curve deviates from the straight line at 2 G and 3 G for the Eu- and Gd-compound, respectively. The narrow region of the full Meissner effect roughly reflects the temperature-dependent lower critical field in the *ab*-plane $B_{c1}^{ab}(T)$. The average lower critical field $B_{c1}^{\rm ave}$ for the bulk sample as determined from the peak of the initial diamagnetic magnetization curves is 7 G for R = Eu and 13 G for R = Gd. The effect on the exact peak value due to the surface barrier pinning is neglected. For $RuSr_2EuCu_2O_8$, $B_{c1}^{\rm ave}$ decreases steadily from 7 G at 2 K to 6 G at 5 K, 4 G at 10 K, and below 1 G at 15 K. A simple empirical parabolic fitting gives $B_{c1}^{\rm ave}(T) = B_{c1}^{\rm ave}(0)[1 - (T/T_{\rm SVS})^2]$, with average $B_{c1}^{\rm ave}(0) \sim 7$ G and the spontaneous vortex state temperature $T_{\rm SVS} = 16$ K. The Ginzburg-Landau anisotropy formula $B_{c1}^{\rm ave} = (2B_{c1}^{ab} + B_{c1}^{c})/3$, then provides an estimated *c*-axis lower critical field $B_{c1}^{c}) \sim 17$ G and anisotropy parameter ~ 8.5.

The lower field superconducting phase diagram for the polycrystalline bulk sample is shown in Fig. 4. The average lower critical field $B_{c1}^{\rm ave}$ separates the Meissner state and vortex state. The upper critical field B_{c2} and vortex melting field $B_{\rm melting}$ determined from the magnetoresistivity measurements are field-independent below 20 G. The WFM-induced internal dipole field $B_{\rm dipole}$ of 8.8 G on the CuO_2 bi-layers is estimated using the extrapolated $B_{c1}^{\rm ave}$ value at $T = 0$, $(B_{c1}^{\rm ave}(0) + B_{\rm dipole})/B_{c1}^{\rm ave}(0) = T_c/_{\rm SVS}$. It further yields a small net spontaneous magnetic moment μ_s of 0.1 μ_B per Ru, based on the relation of $B_{\rm dipole} \sim 2\mu_s/(c/2)^3$, where $c/2 = 0.58$ nm is the distance between the midpoint of the CuO_2 bi-layers and the two nearest-neighbor Ru moments. If the WFM structure is indeed a G-type antiferromagnetic order with 1.5 μ_B for Ru^{5+} in t_{2g} states canted along the

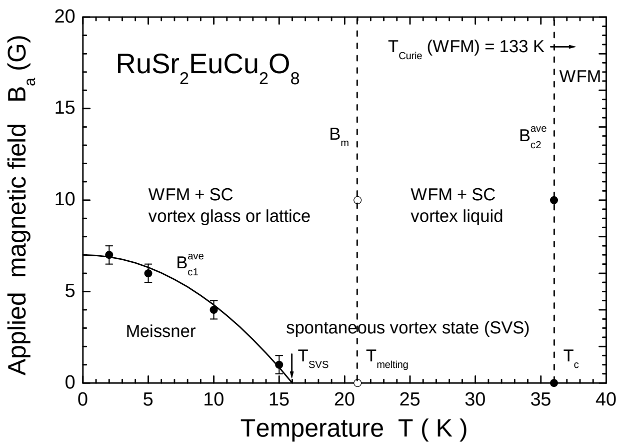

FIG. 4: The low field, low temperature superconducting phase diagram $B_a(T)$ of $RuSr_2EuCu_2O_8$. The spontaneous vortex state (SVS) occurs between $T_{\rm SVS} = 16$ K and $T_{\rm c} = 36$ K. The vortex lattice/glass melting temperature $T_{\rm melting}$ is defined from the temperature at which the resistivity drops to zero.

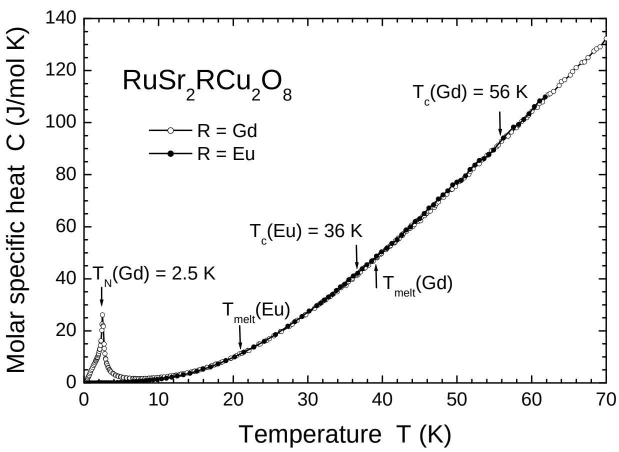

FIG. 5: The molar specific heat of $RuSr_2RCu_2O_8$ (R = Eu, Gd). Antiferromagnetic Gd^{3+} ordering prevails at 2.5 K.

tetragonal basal plane, the small μ_s would give a canting angle of 4° from the tetragonal c-axis and be difficult to be detected in neutron diffraction with a resolution $\sim 0.1\mu_B$.

The molar specific heat data up to 70 K in Fig. 5 show a good agreement between the Eu- and Gd-compounds, except that a peak reflects the antiferromagnetic Gd^{3+} ordering near $T_{\rm N} \sim 2.5$ K. The specific heat jump of superconducting Gd-compounds was reported in the previous report [15, 28]. However, no visible jump in the specific heat was detected near $T_{\rm c} = 36$ K. Specifically, assuming a same magnitude as that observed in $La_{1.85}Sr_{0.15}CuO_4$ (ΔC $\sim$ 0.33 J/mol K at $T_{\rm c} = 37$ K) and $YBa_2Cu_3O_7$ (ΔC $\sim$ 4.6 J/mol K at $T_{\rm c} = 92$ K)

[53], an estimated $\Delta C \sim 1$ J/mol K at T_c is about 1% of the total specific heat, falling below the experimental precision.

It would be of interest to obtain information on the Gd^{3+} ordering. To do so, delineation of various contributions to the total specific heat begins with the nonmagnetic Eu-compound up to 7 K. In the format of C/T versus T^2, the data in Fig. 6 can be well fitted by the sum of four terms with different temperature dependence:

$$C = \beta T^3 + \alpha T^2 + \gamma T + \frac{\eta}{T^2}. \tag{1}$$

The coefficient of the first term, $\beta = 0.89$ mJ/mol K^4, can be used to derive a Debye temperature θ_D of the lattice,

$$\beta = n(12\pi^4/5)N_A k/\theta_D^3, \tag{2}$$

where N_A is Avogadro's number, k the Boltzmann constant, and the number of atoms per formula unit is $n = 14$. The θ_D value of 312 K thus obtained supports the validity of the T^3-dependence approximation in the Debye model for the lattice specific heat below 7 K $\sim \theta_D/50$. The quadratic term has two possible sources: the nodal line excitation for the d-wave pairing symmetry and the spin wave excitation of the WFM Ru sublattice. The fact that the observed α value of 4.2 mJ/mol K is much larger than the 0.1 mJ/mol K of $YBa_2Cu_3O_7$ could be an indication of a less important nodal line excitation, but an enhanced spin wave excitation. The linear term is considered normally as an electronic contribution, which is not expected to exist in a superconductor at any temperature much lower than T_c. While the observed coefficient $\gamma = 7.3$ mJ/mol K^2 is comparable to that of some cuprates, its origin remains to be identified. One plausible explanation is based on the complicated magnetic structure and mixed valence. Such a scenario could lead to a spin glass-like lattice, for which an even larger linear term in specific heat has been observed in another Ru compound, Ba_2PrRuO_6 [54].

The last term with a T^{-2} dependence is most likely the high-temperature tail of a Schottky anomaly. Its occurrence at relatively low temperatures suggests the nuclear energy splittings as being the cause. Such energy splittings occur typically for nuclei having a spin I and magnetic moment μ_n in a hyperfine magnetic field H_{hf}. For the calorimetrical measurements under consideration, they are is most likely associated with the Ru nuclei, since the $4d$ magnetic moments of ordered Ru ions are spatially fixed, polarizing the s-electrons and producing a net spin at the nuclei, yielding a hyperfine field. There are two Ru isotopes with non-zero μ_n: ^{99}Ru (fractional natural abundance A = 0.1276, I = 5/2, and $\mu_n = -0.6413$) and ^{101}Ru (A = 0.1706, I = 5/2, and $\mu_n = -0.7188$) [55]. However, nuclear energy splittings can also be caused by the interaction between the quadrupole moment of a nucleus and the electric field gradient produced by neighboring atoms. The electric field gradient could be quite high in the layered compound. Meanwhile, Cu and Eu or ^{155}Gd (A = 14.7%) and ^{157}Gd (A = 15.7%) nuclei all have a non-zero quadrupole moment. Without the full knowledge of the magnetic hyperfine field and electric field gradient, it is not feasible at present to delineate the experimentally obtained η of 6.63 mJ K/mol into the two different contributions.

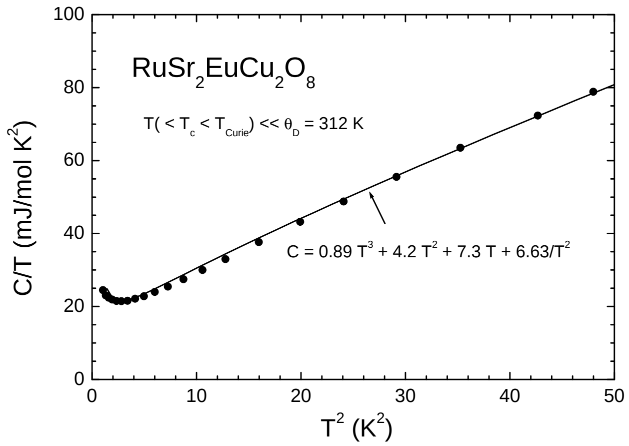

FIG. 6: Low temperature C/T versus T^2 of $RuSr_2EuCu_2O_8$ from 1 K to 7 K. Data above 1 K can be fitted using $C(T) = \beta T^3 + \alpha T^2 + \gamma T + \eta/T^2$ with the Debye temperature $\theta_D = 312$ K.

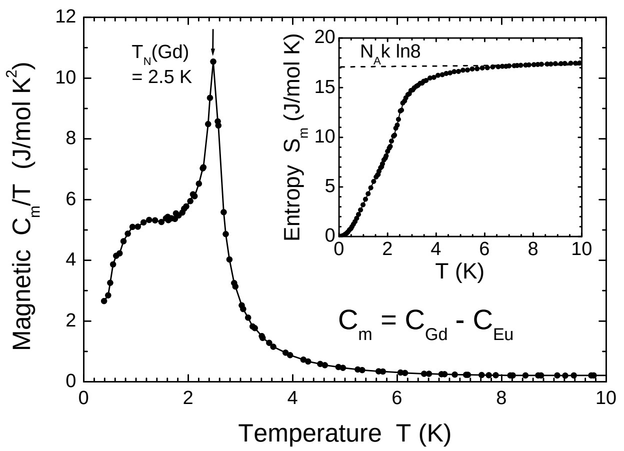

FIG. 7: Temperature dependence of the magnetic specific heat and entropy (inset) associated with Gd^{3+} ordering in $RuSr_2GdCu_2O_8$.

By assuming that its various coefficients in Eq. (1) for the Eu-compound remain the same for the Gd-compound, one can then obtain the magnetic contribution to the specific heat associated with the antiferromagnetic Gd^{3+} ordering as

$$C_m = C_{Gd} - C_{Eu}. \quad (3)$$

The results are shown in Fig. 7. Using the format of C_m/T versus T. It is of interest to note a broad shoulder below T_N, a common feature seemingly prevailing in other similar types of compounds such as $GdBa_2Cu_3O_7$, $GdBa_2Cu_4O_8$, and $TlBa_2GdCu_2O_7$ [56–58]. According to Fishman and Liu [59], it is due to spin fluctuations in the normally ordered state, and such fluctuations are more pronounced for large spins. Indeed, Gd^{3+} has the largest spin among all R^{3+} ions. The areal integral in Fig. 7, including that associated with the broad shoulder should yield the magnetic entropy,

$$S_{\mathrm{m}} = \int (C_{\mathrm{m}}/T)dT. \tag{4}$$

As shown in the inset, S_{m} reaches a saturation value of 17.6 J/mol K around 10 K. Considering the built-in approximation in Eq. (4), this agrees exceptional well with the theoretical value of $N_{\mathrm{A}}k\ln(2J+1) = N_{\mathrm{A}}k\ln 8 = 17.2$ J/mol K for the complete ordering of Gd^{3+}.

IV. CONCLUSION

The lower critical field with $B_{c1}(0) = 7$ G and $T_{\mathrm{SVS}} = 16$ K indicates the existence of a spontaneous vortex state (SVS) between 16 K and T_{c} of 36 K. This SVS state is closely related to the weak-ferromagnetic order with a net spontaneous magnetic moment of $\sim 0.1\ \mu_B$/Ru, which generates a weak magnetic dipole field around 8.8 G in the CuO_2 bi-layers. The vortex melting transition temperature at 21 K obtained from resistivity measurements and the onset of diamagnetic signal indicates a broad vortex liquid region due to the coexistence and interplay between superconductivity and the WFM order. No visible specific heat jump was observed near T_{c} for the Eu- and Gd-compounds. Finally, the magnetic entropy associated with Gd^{3+} antiferromagnetic ordering at 2.5 K is confirmed to be close to $N_{\mathrm{A}}k\ln 8$ for J = S = 7/2.

Acknowledgements

This work was supported by the National Science Council of the R.O.C. under contract Nos. NSC95-2112-M-007-056-MY3 and NSC95-2112-M-032-002.

References

* Electronic address: hcku@phys.nthu.edu.tw

[1] L. Bauernfeind, W. Widder, and H. F. Braun, Physica C **254**, 151 (1995).
[2] L. Bauernfeind, W. Widder, and H. F. Braun, J. Low Temp. Phys. **105**, 1605 (1996).
[3] K. B. Tang, Y. T. Qian, L. Yang, Y. D. Zhao, and Y. H. Zhang, Physica C **282–287**, 947 (1997).
[4] J. L. Tallon *et al.*, IEEE Trans. Appl. Supercond. **9**, 1696 (1999).
[5] C. Bernhard *et al.*, Phys. Rev. B **59**, 14099 (1999).
[6] A. C. McLaughlin, W. Zhou, J. P. Attfield, A. N. Fitch, and J. L. Tallon, Phys. Rev. B **60**, 7512 (1999).
[7] J. L. Tallon, J. W. Loram, G. V. M. Williams, and C. Bernhard, Phys. Rev. B **61**, R6471 (2000).
[8] C. Bernhard, J. L. Tallon, E. Brücher, and R. K. Kremer, Phys. Rev. B **61**, R14960 (2000).

[9] J. W. Lynn, B. Keimer, C. Ulrich, C. Bernhard, and J. L. Tallon, Phys. Rev. B **61**, R14964 (2000).
[10] O. Chmaissem, J. D. Jorgensen, H. Shaked, P. Dollar, and J. L. Tallon, Phys. Rev. B **61**, 6401 (2000).
[11] G. V. M. Williams and S. Krämer, Phys. Rev. B **62**, 4132 (2000).
[12] C. W. Chu *et al.*, Physica C **335**, 231 (2000).
[13] A. C. Mclaughlin, V. Janowitz, J. A. McAllister, and J. P. Attfield, Chem. Commun. (Cambridge) **2000**, 1331 (2000).
[14] X. H. Chen *et al.*, J. Phys. Condens. Matter **12**, 10561 (2000).
[15] J. L. Tallon, J. W. Loram, G. V. M. Williams, and C. Bernhard, Phys. Rev. B **61**, R6471 (2000).
[16] R. L. Meng *et al.*, Physica C **353**, 195 (2001).
[17] V. P. S. Awana *et al.*, Physica C **357–360**, 121 (2001).
[18] D. P. Hai *et al.*, Physica C **357–360**, 406 (2001).
[19] A. P. Litvinchuk *et al.*, Physica C **361**, 234 (2001).
[20] C. T. Lin, B. Liang, C. Ulrich, and C. Berhard, Physica C **364-365**, 373 (2001).
[21] H. Takagiwa, J. Akimitsu, H. Kawano-Furukawa, and H. Yoshizawa, J. Phys. Soc. Jpn. **70**, 333 (2001).
[22] J. D. Jorgensen *et al.*, Phys. Rev. B **63**, 054440 (2001).
[23] R. S. Liu, L.-Y. Jang, H.-H Hung, and J. L. Tallon, Phys. Rev. B **63**, 212507 (2001).
[24] M. Požek, A. Dulčić, D. Paar, G. V. M. Williams, and S. Krämer, Phys. Rev. B **64**, 064508 (2001).
[25] V. G. Hadjiev *et al.*, Phys. Rev. B **64**, 134304 (2001).
[26] Y. Tokunaga *et al.*, Phys. Rev. Lett. **86**, 5767 (2001).
[27] P. W. Klamut, B. Dabrowski, S. Kolesnik, M. Maxwell, and J. Mais, Phys. Rev. B **63**, 224512 (2001).
[28] X. H. Chen *et al.*, Phys. Rev. B **63**, 64506 (2001).
[29] B. Lorenz, Y. Y. Xue, R. L. Meng, and C. W. Chu, Phys. Rev. B **65**, 174503 (2002).
[30] T. P. Papageorgiou, H. F. Braun, and T. Herrmannsdörfer, Phys. Rev. B **66**, 104509 (2002).
[31] H. Fujishiro, M. Ikebe, and T. Takahashi, J. Low Temp. Phys. **131**, 589 (2003).
[32] C. Shaou, H. F. Braun, and T. P. Papageorgiou, J. Alloys and Compounds **351**, 7 (2003).
[33] A. Vecchione *et al.*, Int. J. Mod. Phys. B **17**, 899 (2003).
[34] F. Cordero, M. Ferretti, M. R. Cimberle, and R. Masini, Phys. Rev. B **67**, 144519 (2003).
[35] H. Sakai, N. Osawa, K. Yoshimura, M. Fang, and K. Kosuge, Phys. Rev. B **67**, 184409 (2003).
[36] Y. Y. Xue, F. Chen, J. Cmaidalka, R. L. Meng, and C. W. Chu, Phys. Rev. B **67**, 224511 (2003).
[37] J. E. McCrone *et al.*, Phys. Rev. B **68**, 064514 (2003).
[38] A. López, I. Souza Azevedo, J. E. Musa, E. Baggio-Saitovitch, and S. G. García, Phys. Rev. B **68**, 134516 (2003).
[39] S. García, J. E. Musa, R. S. Freitas, and L. Ghivelder, Phys. Rev. B **68**, 144512 (2003).
[40] T. P. Papageorgiou, H. F. Braun, T. Görlach, M. Uhlarz, and H. v. Lohneysen, Phys. Rev. B **68**, 144518 (2003).
[41] V. P. S. Awana, T. Kawashima, and E. Takayama-Muromachi, Phys. Rev. B **67**, 172502 (2003).
[42] P. W. Klamut *et al.*, Physica C **387**, 33 (2003).
[43] T. Nachtrab, D. Koelle, R. Kleiner, C. Bernhard, and C. T. Lin, Phys. Rev. Lett. **92**, 117001 (2004).
[44] Y. Y. Xue *et al.*, Physica C **408-410**, 638 (2004).
[45] S. García and L. Ghivelder, Phys. Rev. B **70**, 052503 (2004).

[46] C. J. Liu *et al.*, Phys. Rev. B **71**, 014502 (2004).
[47] C. Y. Yang, B. C. Chang, H. C. Ku, and Y. Y. Hsu, Phys. Rev. B **72**, 174508 (2005).
[48] T. P. Papageorgiou *et al.*, Euro. Phys. J. B **52**, 383 (2006).
[49] Y. C. Lin *et al.*, Intern. J. Mod. Phys. B **19**, 339 (2005).
[50] T. Y. Chiu *et al.*, Chin. J. Phys. **43**, 616 (2005).
[51] H. C. Ku *et al.*, J. Appl. Phys. **97**, 10B110 (2005).
[52] B. C. Chang, C. Y. Yang, Y. Y. Hsu, B. N. Lin, and H. C. Ku AIP conference proceeding **850**, 677 (2006).
[53] C. P. Poole, Jr., H. A. Farach, and R. J. Creswick, *Superconductivity* (Academic Press, Inc. San Diego, 1995), Chap. 4.
[54] S. M. Rao *et al.*, Phys. Lett. A **324**, 71 (2004).
[55] *CRC Handbook of Chemistry and Physics*, 86th ed., Taylor and Francis, (2005-2006).
[56] S. E. Brown *et al.*, Phys. Rev. B. **36**, 2298 (1987).
[57] J. C. Ho *et al.*, Physica C **282-287**, 1403 (1997).
[58] Y. Y. Chen, C. C. Lai, B. S. Chiou, J. C. Ho, and H. C. Ku, Phys. Rev. B **47**, 12178 (1993).
[59] R. S. Fishman and S. H. Liu, Phys. Rev. B **40**, 11028 (1989).